Proteins (Clementi, E., Corongui, G., Sarma, M. H., Sarma, R. H., Eds.) pp 485–495, Adenine Press, Guilderland, NY.
Schevitz, R. W., Otwinowski, Z., Joachimiak, A., Lawson, C. L., & Sigler, P. B. (1985) *Nature (London) 317*, 782–786.
Simons, A., Tils, D., von Wilcken-Bergmann, B., & Müller-Hill, B. (1984) *Proc. Natl. Acad. Sci. U.S.A. 81*, 1624–1628.
States, D. J., Haberkorn, R. A., & Ruben, D. J. (1982) *J. Magn. Reson. 48*, 286–297.
van Boom, J. H., Burgers, P. H. J., & van Deursen, P. H. (1976) *Tetrahedron Lett.*, 869–872.
Weber, I. T., Mckay, D. B., & Steitz, T. A. (1982) *Nucleic Acids Res. 10*, 5085–5102.
Winter, R. B., Berg, O. G., & von Hippel, P. H. (1981) *Biochemistry 20*, 6961–6977.
Wolberger, C., Dong, Y., Ptashne, M., & Harrison, S. C. (1988) *Nature (London) 335*, 789–795.
Wüthrich, K. (1986) in *NMR of proteins and nucleic acids*, Wiley, New York.

Proton NMR Studies of a Metallothionein from *Neurospora crassa*: Sequence-Specific Assignments by NOE Measurements in the Rotating Frame†

J. A. Malikayil,‡ Konrad Lerch,§ and Ian M. Armitage*,‡

Departments of Molecular Biophysics and Biochemistry and of Diagnostic Radiology, Yale University School of Medicine, P.O. Box 3333, New Haven, Connecticut 06510, and Biochemisches Institut, Universität Zürich, Winterthurerstrasse 1, CH-8057 Zürich, Switzerland

Received September 13, 1988; Revised Manuscript Received December 6, 1988

ABSTRACT: Sequential ^{1}H NMR assignments of a metallothionein from *Neurospora crassa* have been accomplished by the combined use of COSY, 2QF-COSY, HOHAHA, and rotating-frame NOE experiments. All potentially observable resonances were assigned except for the ϵ-NH_3 group of the C-terminal lysine. ^{1}H NOEs, when observed in the laboratory frame and at 500-MHz spectrometer frequency, were negligible in this protein due to the inherent rotational correlation time of the molecule. This difficulty was circumvented by measuring transverse NOEs in the rotating frame under spin-locking conditions. The observed pattern of NOEs reveals a marked absence of "regular" secondary structures in the protein. Thus, the stability of this metallothionein's tertiary structure must arise primarily from its metal ligation. This appears to be a general feature of MTs since a general lack of extensive secondary structural elements was also observed in other metallothioneins.

Metallothionein from the fungus *Neurospora crassa* (NMT) is the smallest known metallothionein (MT). The protein contains 25 amino acid residues and has a molecular weight (M_r) of 2200. When isolated from mycelia that were exposed to high levels of Cu, NMT contains 6 mol of Cu(I)/mol of protein in thiolate ligation to seven cysteine residues (Beltramini & Lerch 1986). The positions of all seven cysteines are identical with those of the first seven cysteines of the N-terminal region (β domain) of hepatic mammalian MTs. However, NMT binds exclusively Cu(I) in its physiological state in contrast to the β domain of mammalian MTs that are known to accommodate a variety of heavy metal ions (Kägi & Vallee, 1961). Both NMR and X-ray diffraction methods have been used to elucidate the 3D structure of two mammalian MTs (Frey et al., 1985; Braun et al., 1986; Vasak et al., 1987; Furey et al., 1986). A comparable wealth of structural information is not yet available for NMT or for MTs from lower organisms. With the objective to obtaining the same, we have conducted a two-dimensional ^{1}H NMR study of NMT. Of particular interest was the elucidation of the three-dimensional solution structural features of NMT that attribute this protein with its exclusive in vivo specificity for Cu(I). In this paper we describe the complete sequence-specific ^{1}H NMR resonance assignments of the protein.

The use of the conventional two-dimensional nuclear Overhauser experiment (2D NOESY) in this study proved unsuccessful in providing ^{1}H NOEs for sequential resonance assignments. This results from the fact that the tumbling rate τ_c of this protein is such that $\omega\tau_c \sim 1$ at a spectrometer frequency of 500 MHz which results in negligible ^{1}H–^{1}H NOEs in the laboratory frame. Therefore, we used the 2D CAMELSPIN experiment to measure transverse NOEs in the rotating frame under spin-locking conditions (Bothner-By et al., 1984). In the rotating frame, NOEs are always positive and increase with increasing correlation time of the molecule. Rotating-frame NOEs have the additional advantage that the spin-diffusion effects are smaller than those in NOESY spectra (Bothner-By et al., 1984).

Experimental Procedures

Sample Preparation. NMT contains six diamagnetic Cu(I) centers that are susceptible to facile oxidation to the paramagnetic Cu(II) state in the presence of oxygen. The presence of Cu(II) ions can severely hamper the NMR analysis because of line broadening and the consequent quenching of proton NOEs by paramagnetic relaxation. Therefore, special precautions were taken to safeguard the protein from exposure

† This work was supported by a grant from the National Institute of Health, DK 18778, and benefited from instrumentation provided through the shared instrumentation program of the Division of Research Resources of NIH, RR 03475, the Biological Instrumentation Program of the National Science Foundation, DMB 8610557, and the American Cancer Society, RD259. The support of a Swiss National Science grant to K.L. is also acknowledged.

‡ Yale University School of Medicine.
§ Universität Zürich.

0006-2960/89/0428-2991$01.50/0

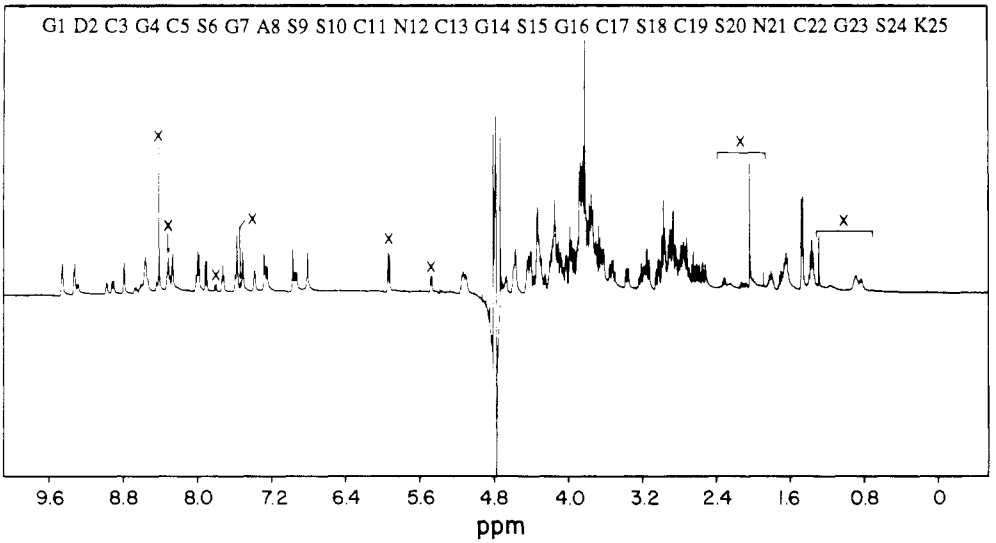

FIGURE 1: One-dimensional ^1H NMR spectrum of NMT. X denotes resonances from impurities in the sample (see text). The amino acid sequence of the protein is shown at the top.

to oxygen and paramagnetic ions.

All solutions that were used in the sample preparation were thoroughly purged of oxygen by repeated evacuation/flushing cycles using a vacuum/argon manifold. All sample manipulations were carried out in this anaerobic environment. NMT was lyophilized from 5 mL of 20 mM potassium phosphate buffer at pH 7.5. The lyophilized protein was dissolved in a H_2O/D_2O (60%/40% v/v) solvent mixture containing approximately 3 mM β-mercaptoethanol. The protein sample was treated with 100 mg of Chelex-100 resin and was then transferred into an NMR tube by way of an online filter–syringe assembly. The NMR tube was promptly sealed under a gentle flow of Ar. The final protein concentration was calculated to be ~8 mM.

The 1D ^1H NMR spectrum of the sample shown in Figure 1 is well resolved and provides no evidence for paramagnetic line broadening. The NMR spectrum of a test sample that was prepared by an identical procedure remained unchanged over a period of 3 months at room temperature. Thus, the protein demonstrated remarkable stability under our experimental conditions, and all spectra reported in this paper were collected with the same sample. Resonances labeled "X" could be confidently assigned to contaminants in the sample because these resonances do not show scalar couplings in COSY spectra that are characteristic of the amino acids present in the protein.

NMR Spectroscopy. All spectra were collected at 25 °C on a Bruker AM 500-MHz NMR spectrometer equipped with an Aspect 3000 computer and a digital phase shifter. Chemical shifts are quoted relative to external 3-(trimethylsilyl)-[2,2,3,3-D_4]propionate, with downfield shifts defined as positive. The time domain signals were transferred onto a VAX-750 computer for data processing using the FTNMR software package (Hare Reseach, Inc.). In all cases, a soft presaturation pulse was employed for solvent suppression during the relaxation delay (1.5 s). A spectral width of 5320 Hz and a corresponding incrementation time of 94 μs were applied in all cases. All spectra were acquired in the phase-sensitive mode by the method of time proportional phase incrementation (Redfield & Kuntz, 1975; Bodenhausen et al., 1980) as described by Marion and Wüthrich (1983).

In COSY and 2QF-COSY experiments, 512 t_1 points were sampled. Each t_1 point consisted of 160 transients of 2048 complex points. The filter delay for the 2QF-COSY was 3 μs. In both cases, the F_1 dimension was zero-filled to 2048 points prior to the second Fourier transform. In the COSY spectrum, a sine bell was applied along both dimensions, and a cubic spline base-line correction was applied to each row after the first transform. For the 2QF-COSY spectrum, a 30° shifted sine bell was applied along both axes, and no base-line correction was employed.

Two 2D HOHAHA (HOmonuclear HArtman HAhn) spectra (Bax & Davis, 1985) were acquired with mixing periods of 17 and 56 ms. A MLEV-17 composite pulse was used for the isotropic mixing, and a Z-filter was inserted at either ends of the mixing pulse to overcome spectral phase anomalies (Rance, 1987). A total of 512 t_1 points averaging 256 transients of 1024 complex points were sampled. After Fourier transform in the F_2 dimension, each row was subjected to a five-point polynomial base-line correction. The F_1 dimension was zero-filled to 1024 real points before the second Fourier transform, resulting in a final 1K by 1K data matrix.

2D rotating-frame nuclear Overhauser effect spectra (Bothner-By et al., 1984) were acquired with mixing periods of 10, 40, 90, and 150 ms. The spin-locking pulse (excitation bandwidth of 6 kHz) consisted of a repeating series of 180° pulses (100 μs) of constant phase separated by a 100-μs fixed delay. The fixed delays between the spin-locking pulses were a precautionary measure to safeguard the probe from excessive heating. A pair of Z-filters with a delay of 3 μs were inserted on either ends of the spin-locking pulse as in the case of HOHAHA spectra. For processing, a 30°-shifted sine bell window was applied along both dimensions. A five-point polynomial base-line correction was applied to each row after the first Fourier transform, and the F_1 dimension was zero-filled to 2048 points before the second Fourier transform.

Results and Discussion

Identification of Spin Systems. NMT contains only 7 of the 20 common amino acids (Figure 1). Despite the high degree of amino acid degeneracy, ^1H NMR spectra of the protein showed good resolution. In only one case, G1 and G14, was there degeneracy in the NH and $C^\alpha H$ chemical shifts.

In the 2QF-COSY spectrum, Figure 2, the single alanine spin system could be easily identified by the scalar coupling of its $C^\alpha H$ proton to a doublet at 1.47 ppm. The extended spin system of the single lysine could be followed in the same spectrum. All six glycines were identified by the large geminal couplings of their $C^\alpha H$ protons in the 2QF-COSY spectrum. This assignment was confirmed for five glycines by the distinctive pairs of NH–$C^\alpha H$ crosspeaks in the COSY spectrum,

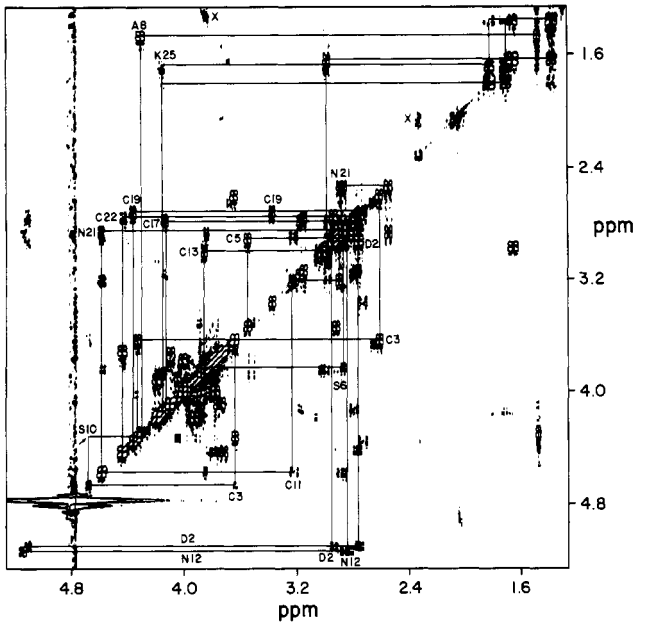

FIGURE 2: An expansion of the 2QF-COSY spectrum showing the $C^{\alpha}H$ and the side-chain regions. Both positive and negative contours are drawn.

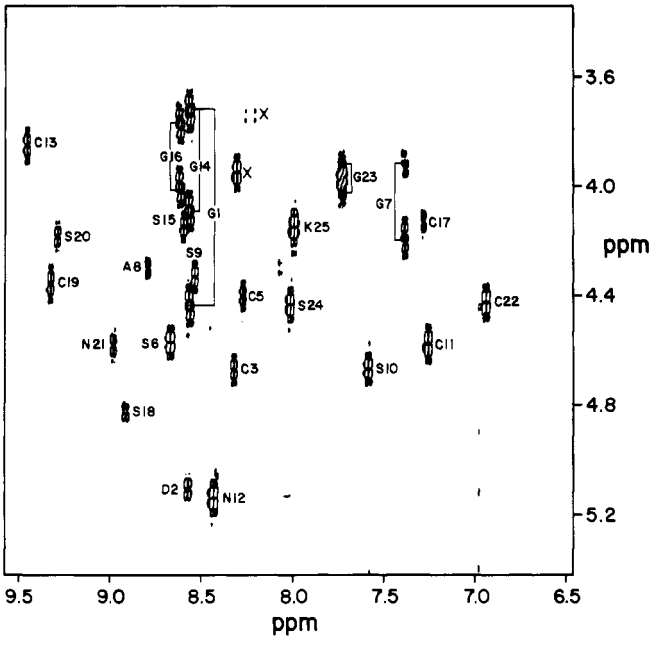

FIGURE 3: Fingerprint region of the COSY spectrum. Both positive and negative contours are shown. Constructs identify five of the six glycines, and X identifies impurities.

Figure 3. Neither NH–$C^{\alpha}H$ crosspeak from the remaining glycine, G4, was observed in the COSY and 2QF-COSY spectra. However, these crosspeaks were observed in the 10-ms CAMELSPIN and 17-ms HOHAHA spectra. The seven serine spin systems were distinguished on the basis of the larger chemical shifts of their $C^{\beta}H_2$ resonances compared to those of asparagine, aspartic acid, and cysteine. The $C^{\alpha}H$–$C^{\beta}H$ crosspeaks of two serines, S10 and S18, were not observed in the COSY and 2QF-COSY spectra. These crosspeaks were identified in the HOHAHA spectra. Distinction among the remaining spin systems, seven cysteines, two asparagines, and one aspartic acid, was not possible at this early stage of the analysis. For the majority of spin systems, extended NH–$C^{\alpha}H$–$C^{\beta}H$ and $C^{\alpha}H$–$C^{\beta}H$–$C^{\beta'}H$ connectivities were observed in the 57-ms HOHAHA spectrum.

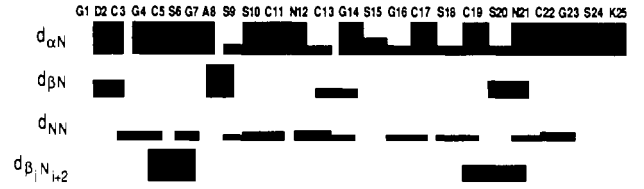

FIGURE 4: Summary of the observed transverse NOEs in NMT. The thickness of the bars corresponds to NOE intensities grouped into four classes by visual inspection.

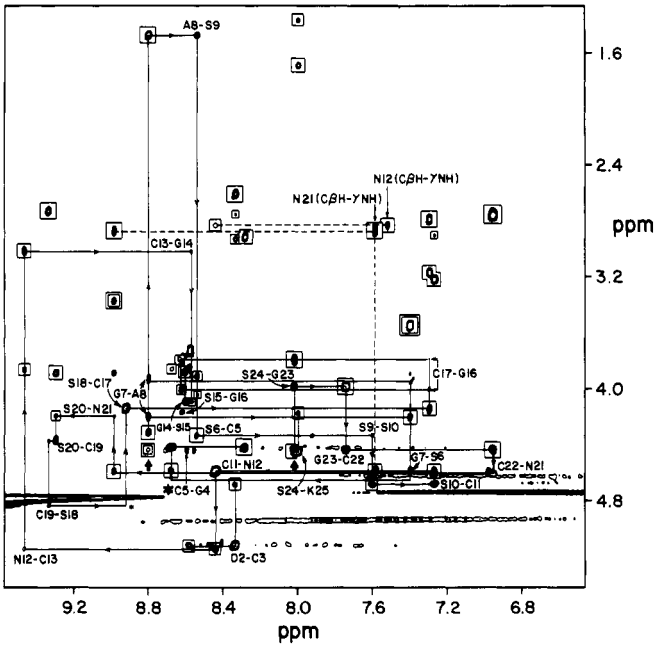

FIGURE 5: Sequential assignments in NMT. An expansion of the 150-ms CAMELSPIN spectrum is displayed. For the majority of residues, assignments were made by $d_{\alpha N}$ NOEs and confirmed in certain cases by d_{NN} NOEs. A8–S9 sequential assignment was based exclusively on a $d_{\beta N}$ NOE (broken lines). C13–G14 assignment was based on both $d_{\beta N}$ and d_{NN} NOEs.

Sequential Resonance Assignments. NOEs were designated following the notations of Wüthrich et al. (1984). In the 150-ms 2D CAMELSPIN spectrum of NMT, 20 $d_{\alpha N}(i,i+1)$, 4 $d_{\beta N}(i,i+1)$, 11 $d_{NN}(i,i+1)$, and 4 $d_{\beta N}(i,i+2)$ NOEs were identified. The intensity of the observed transverse NOEs was grouped into four categories by visual inspection. A summary of the observed NOEs is presented in Figure 4. The connectivity between C3 and G4 was based on the d_{NN} NOE, that between A8 and S9 was based on the $d_{\beta N}$ NOE, and that between C13 and G14 was based on both $d_{\beta N}$ and d_{NN} NOEs. In all other cases, sequential assignments were based on $d_{\alpha N}$ NOEs with the other types of NOEs, when observed, corroborating the assignments.

The sequential assignments of NMT are presented in Figures 5 and 6, the two unique residues A8 and K25 being used as starting points. These starting points are indicated with thick arrows in Figure 5. Starting at the C-terminal K25, residues 25–15 were assigned by a continuous stretch of $d_{\alpha N}$ NOEs. Due to the near degeneracy of the NH resonances of S24 and K25, their $d_{\alpha N}$ NOE crosspeak could not be resolved from the intraresidue NH–$C^{\alpha}H$ NOE crosspeak of S24. However, the composite nature of this crosspeak is evident from its large line width along the F_2 dimension in comparison to that of the corresponding NH–$C^{\alpha}H$ crosspeak of S24 in the HOHAHA spectrum. Remaining assignments within the segment S15–K25 proceeded without difficulty. The second step of the sequential analysis started at the unique alanine residue. A8–S9 connectivity was established by a strong $d_{\beta N}$

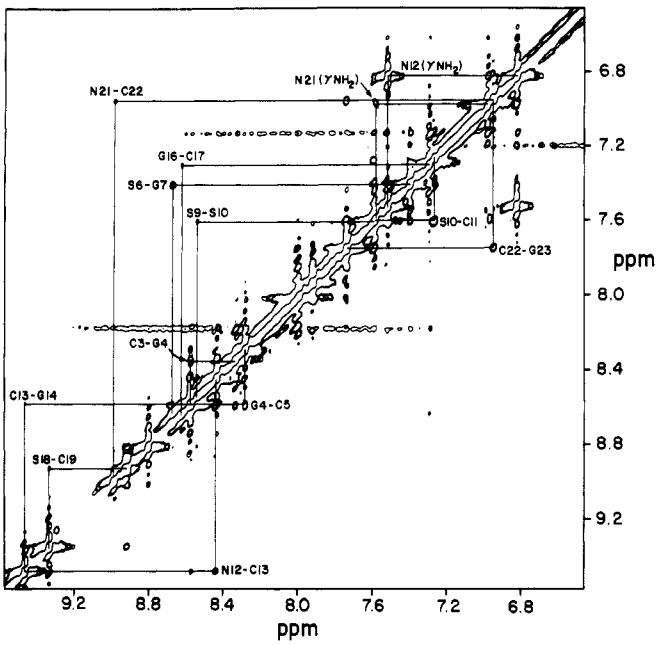

FIGURE 6: Expansion of the 150-ms CAMELSPIN spectrum showing the NH–NH connectivities. C3–G4 sequential assignment was based exclusively on the d_{NN} NOE.

NOE. Residues 9–13 were assigned by $d_{\alpha N}$ NOEs. C13–G14 connectivity was obtained from both $d_{\beta N}$ and d_{NN} NOEs. G14–S15 connectivity was established by the $d_{\alpha N}$ NOE, joining this segment of the protein to the S15–K25 region that had been previously assigned. In the third step of the analysis, sequential assignments proceeded from A8 toward the N-terminus. Residues G4–A8 were assigned by strong $d_{\alpha N}$ NOEs. The d_{NN} NOE crosspeaks connected C5 to G4 and G4 to C3. The $d_{\alpha N}$ crosspeak between G4 and C5 was slightly shifted in the F_1 dimension as denoted by the asterisk in Figure 5. However, this NOE crosspeak was unambiguously identified in the CAMELSPIN spectrum with a 10-ms mixing time. In this context, it is noteworthy that the NH–C$^{\alpha}$H crosspeaks of G4 were not observed in COSY spectra, but only in the HOHAHA spectrum collected with a short mixing period. A strong $d_{\alpha N}$ NOE was observed between D2 and C3. Since no NOE was observed between G1 and D2, G1 was assigned by elimination to complete the sequential assignment of NMT. The chemical shifts values of all 25 residues of NMT are presented in Table I.

Assignments of the γ-NH$_2$ Groups of Asparagines. The crosspeaks due to the scalar couplings of the side-chain NH$_2$ protons of N12 and N21 were identified in the HOHAHA spectrum. The corresponding transverse NOE crosspeaks are indicated in Figure 5 where in each case the transverse NOE of one of these protons to one of the C$^{\beta}$H$_2$ protons is indicated by broken lines.

Comments on the Tertiary Structure of NMT. Despite the high degree of amino acid multiplicity, the ^{1}H NMR spectrum of NMT is well resolved. For 15 of the 17 AMX spin systems and for the C-terminal lysine, the C$^{\beta}$H$_2$ resonances were resolved. This dispersion of resonances is indicative of a unique average conformation within a set of rapidly interconverting conformers on the time scale of the proton chemical shifts. However, with the exception of sequential residues, the solution conformation of NMT results in few additional short-range ^{1}H–^{1}H contacts, consistent with the general lack of "regular" secondary structures in this protein. The absence of extensive regular secondary structures was also reported for mammalian MTs (Braun et al., 1986; Furey et al., 1986). The only

Table I: Proton Resonance Assignments for the 25 Residues of NMT

	chemical shift (ppm)			
residue	NH	α	β	others
G1	8.56	4.43, 3.71		
D2	8.57	5.10	2.94, 2.75	
C3	8.33	4.67	3.64, 2.61	
G4	8.58	4.09, 3.73		
C5	8.27	4.40	3.54, 2.93	
S6	8.67	4.57	3.84, 2.86	
G7	7.38	4.19, 3.92		
A8	8.78	4.30	1.48	
S9	8.53	4.34	4.01, 3.91	
S10	7.58	4.67	4.32, 3.65	
C11	7.25	4.58	3.21, 2.89	
N12	8.43	5.13	2.89, 2.84	NH_2 7.52, 6.81
C13	9.45	3.85	3.02	
G14	8.56	4.09, 3.71		
S15	8.60	4.15	3.86	
G16	8.61	4.00, 3.77		
C17	7.28	4.14	3.18, 2.78	
S18	8.91	4.82	4.10, 3.77	
C19	9.32	4.36	3.37, 2.72	
S20	9.29	4.18	3.87, 3.52	
N21	8.97	4.57	2.87, 2.54	NH_2 7.57, 6.98
C22	6.93	4.43	3.14, 2.76	
G23	7.72	4.00, 3.95		
S24	8.01	4.43	3.80, 3.52	
K25	7.98	4.15	1.81, 1.69	1.37 (δ), 1.66 (δ), 2.98 (ϵ)

nonsequential NOEs in the protein were four $d_{\beta_i N_{i+2}}$ (Figure 4) and a long-range NOE between the NH proton of A8 and the C$^{\alpha}$H proton of G1, C22, or S24 (the latter three residues have degenerate C$^{\alpha}$H chemical shifts). The observed pattern of sequential $d_{\alpha N}$ NOEs and the absence of nonsequential NOEs are indicative of a general extended-chain conformation (Wüthrich et al., 1984). Peptide turns of type I, type I′, type II, type II′, and half-turn, however, cannot be ruled out because their characteristic nonsequential NOEs are expected to be weak (Wagner et al., 1986) and thereby elude detection.

The current NOE data provide too few constraints to predict the three-dimensional solution structure of the protein. However, the single long-range NOE from A8 might be indicative of a loop structure in NMT. A 5-Å approach, an approximate upper-bound distance for NOE crosspeaks, between A8 and C22, S24, or G1 could be accommodated by an ω loop (Leszczynski & Rose, 1986). The metal sites on the inside of such a loop with interstrand thiolate ligations would be expected to provide its stability. Such a loop could potentially accommodate a "compact" copper–thiolate cluster as reported by EXAFS analysis (Smith et al., 1986) or a linear copper–thiolate arrangement that was proposed on the basis of other spectroscopic studies (Lerch, 1980; Beltramini & Lerch, 1983).

Thus, additional structural constraints are required to determine the 3D solution structure of this protein. In the case of MT-2 from rabbit liver, metal–cysteine connectivities obtained from heteronuclear multiple quantum correlation experiments served as critical distance constraints for its structure determination (Frey et al., 1985; Live et al., 1985). The native metal of NMT, Cu(I), is unsuitable for similar experiments because of its large quadrupole moment (I = 5/2) and its insensitivity for NMR detection. However, it has been reported in a related MT from yeast that the native Cu(I) sites can be replaced in vitro with Ag(I) ions (I = 1/2) with retention of the same metal to protein stoichiometry (Winge et al., 1985). If this metal substitution is also possible with NMT, heteronuclear multiple quantum experiments analogous to those used for the Cd_7 mammalian MT (Frey et al., 1985) will become feasible and be used to obtain the desired distance

constraints required for the elucidation of the solution structure of NMT.

ACKNOWLEDGMENTS

We thank Dr. Bruce A. Johnson for the use of his graphics terminal emulation software (TERMULATOR).

REFERENCES

Balaram, P., Bothner-By, A. A., & Dadok, J. (1972) *J. Am. Chem. Soc. 94*, 4015.
Bax, A., & Davis, D. G. (1985) *J. Magn. Reson. 65*, 355–366.
Beltramini, M., & Lerch, K. (1983) *Biochemistry 22*, 2043–2048.
Beltramini, M., & Lerch, K. (1986) *Environ. Health Perspect. 65*, 21–27.
Bodenhausen, G., Vold, R. L., & Vold, R. R. (1980) *J. Magn. Reson. 37*, 93–106.
Bothner-By, A. A., Stephens, R. L., & Lee, J. (1984) *J. Am. Chem. Soc. 106*, 811–813.
Braun, W., Wagner, G., Worgotter, E., Vasak, M., Kägi, J. H. R., & Wüthrich, K. (1986) *J. Mol. Biol. 187*, 125–129.
Frey, M. H., Wagner, G., Vasak, M., Sorenson, O., Neuhaus, D., Worgotter, E., Kägi, J. H. R., Ernst, R. R., & Wüthrich, K. (1985) *J. Am. Chem. Soc. 107*, 6847–6851.
Furey, W. F., Robbins, A. H., Clancy, L. L., Winge, D. R., Wang, B. C., & Stout, C. D. (1986) *Science 231*, 704–710.
Kägi, J. H. R., & Vallee, B. L. (1961) *J. Biol. Chem. 236*, 2435–2442.
Lerch, K. (1980) *Nature 284*, 368–370.
Leszczynski, J. F., & Rose, G. D. (1986) *Science 234*, 849–855.
Live, D., Armitage, I. M., Dalgarno, D. C., & Cowburn, D. (1985) *J. Am. Chem. Soc. 107*, 1775–1777.
Marion, D., & Wüthrich, K. (1983) *Biochem. Biophys. Res. Commun. 113*, 967–974.
Otvos, J. D., & Armitage, I. M. (1980) *Proc. Natl. Acad. Sci. U.S.A. 77*, 7094.
Rance, M. (1987) *J. Magn. Reson. 74*, 557–564.
Redfield, A. G., & Kuntz, S. D. (1975) *J. Magn. Reson. 19*, 250–254.
Smith, T. A., Lerch, K., & Hodgson, K. O. (1986) *Inorg. Chem. 25*, 4677–4680.
Vasak, M., Worgotter, E., Wagner, G., Kägi, J. H. R., & Wüthrich, K. (1987) *J. Mol. Biol. 196*, 711–719.
Wagner, G., Neuhaus, D., Worgotter, E., Vasak, M., Kägi, J. H. R., & Wüthrich, K. (1986) *J. Mol. Biol. 187*, 131–135.
Winge, D. R., Neilson, K. B., Gray, W. R., & Hamer, D. H. (1985) *J. Biol. Chem. 260*, 14464–14470.
Wüthrich, K., Billeter, M., & Braun, W. (1984) *J. Mol. Biol. 180*, 715–740.

Conformation Change of the Intestinal Calcium-Binding Protein Induced by Phospholipids in the Presence and Absence of Ca^{2+}

Kenzo Chiba* and Tetsuro Mohri

Second Division, Research Laboratory for Development of Medicine, School of Pharmacy, Hokuriku University, Kanagawa-machi, Kanazawa, Ishikawa 920-11, Japan

Received July 21, 1988; Revised Manuscript Received November 28, 1988

ABSTRACT: Effects of phospholipids (PL's) and lyso-PL's on the conformation of the porcine intestinal calcium-binding protein (CaBP) were studied fluorometrically with 1-(dimethylamino)naphthalene-5-sulfonyl- (DNS-) labeled CaBP. The fluorescence intensity of DNS-labeled CaBP was much higher in the presence of excess EGTA than in its Ca^{2+}-bound state. In the absence of free Ca^{2+} (with 1 mM EGTA) the fluorescence of the labeled CaBP was greatly enhanced by addition of lysophosphatidylcholine (lyso-PC), lysophosphatidylserine (lyso-PS), or lysophosphatidylinositol (lyso-PI). With addition of 25 μM Ca^{2+} the enhancement of the fluorescence by these lyso-PL's was depressed; especially that due to lyso-PC became small. Lysophosphatidylethanolamine (lyso-PE), phosphatidylcholine (PC), phosphatidylserine (PS), phosphatidylinositol (PI), phosphatidylethanolamine (PE), and mono- and dipalmitoylglycerols had no or much less effect on the fluorescence in the presence and absence of Ca^{2+}. Lyso-PC attenuated in a concentration-dependent manner the quenching of the fluorescence of the DNS–CaBP by high temperatures and increase of ionic strength in the presence of EGTA. Lyso-PL's generally protected the CaBP from digestion with proteases in the presence of EGTA. These experimental results suggest that particular lyso-PL's have Ca^{2+}-sensitive interaction with the porcine CaBP and induce conformation change of the CaBP molecules.

The porcine intestinal CaBP[1] was first reported by Hitchman et al. (1972). We previously demonstrated by a quantitative determination of Ca^{2+} binding and measurement of Ca^{2+}-induced changes in the intrinsic fluorescence, CD, and UV absorption that the CaBP molecule has two noncooperative Ca^{2+}-binding sites with essentially the same affinity for Ca^{2+} (Chiba et al., 1983a,b) and increases α-helix content of it by about 5% on maximal binding of Ca^{2+} (Chiba et al., 1983b).

Wasserman (1970) has reported that lyso-PC interacts with the chick CaBP and releases bound Ca^{2+} from the protein. He also suggested that interaction of the CaBP with the intestinal membrane components affects its Ca^{2+} binding and plays an important role in the process of Ca^{2+} absorption. We previously suggested that the porcine CaBP changes its conformation on binding Ca^{2+} so as to increase hydrophobicity in

[1] Abbreviations: CaBP, calcium-binding protein; DNS, 1-(dimethylamino)naphthalene-5-sulfonate; ANS, 1-anilinonaphthalene-8-sulfonate; PC, phosphatidylcholine; PE, phosphatidylethanolamine; PS, phosphatidylserine; PI, phosphatidylinositol; BAEE, N^{α}-benzoyl-L-arginine ethyl ester; CD, circular dichroism; Tris-HCl, tris(hydroxymethyl)aminomethane hydrochloride; SDS, sodium dodecyl sulfate.

0006-2960/89/0428-2995$01.50/0